An Opto-mechanical Probe for Combining Atomic Force Microscopy and Optical Near-Field Surface Analysis

C.H. van Hoorn[1], D.C. Chavan[1], B. Tiribilli[2], G. Margheri[2], A.J.G. Mank[3], F.Ariese[1], and D. Iannuzzi[1]

[1]Department of Physics and Astronomy and Laserlab Amsterdam, VU University, Amsterdam, The Netherlands
[2]Institute of Complex Systems, National Research Council, Sesto Fiorentino, Italy
[3]Philips Innovation Services, Eindhoven, The Netherlands

December 3, 2015

Abstract

We have developed a new easy-to-use probe that can be used to combine atomic force microscopy (AFM) and scanning near-field optical microscopy (SNOM). We show that, using this device, the evanescent field, obtained by total internal reflection conditions in a prism, can be visualized by approaching the surface with the scanning tip. Furthermore, we were able to obtain simultaneous AFM and SNOM images of a standard test grating in air and in liquid. The lateral resolution in AFM and SNOM mode was estimated to be 45 nm and 160 nm, respectively. This new probe overcomes a number of limitations that commercial probes have, while yielding the same resolution.

Scanning probe microscopy (SPM) instruments are widely recognized as valuable tools for characterizing physical, chemical, electrical, electrochemical and optical properties of materials at the nanometer scale. Atomic force microscopy (AFM), for example, is routinely used to map the surface topography with a resolution well beyond the optical limit, both in gaseous and liquid environments [1]. By replacing the standard AFM cantilever with a tipped glass fiber, one can then equip the instrument with scanning near-field optical microscopy (SNOM) capabilities. The latter can provide information on the optical field emerging from the surface of the sample with a lateral resolution of a few tens of nanometers [2, 3, 4]. The combination of AFM and SNOM has found applications in many fields, including cell biology and single molecule experiments [5, 6].

Unfortunately, current AFM+SNOM probes come with some limitations. In the most widely used setups, the scanning fiber is glued to one of the two prongs of a piezoelectric tuning fork, which cannot be immersed in conductive liquids [3]. To obtain an image of a solid surface in a liquid environment, one thus needs to ensure the tuning fork is kept out of the immersion bath [5]. In this configuration, the meniscus of the liquid on the fiber may influence the performance of the probe. Furthermore, tuning forks cannot be used in contact with the sample, hampering any possibility to perform contact mode scanning. This restriction can be overcome by replacing the probe with a tipped fiber bent in the form of a cantilever. The position of the cantilever can then be monitored via an optical triangulation readout [7]. Alternatively, a standard silicon AFM cantilever can be modified for near-field imaging by making a small hole at the tip apex [**?**]. These configurations also facilitate experiments in liquids, but add the nuisance of the alignment procedure of the readout, which becomes even more tedious when the probe is immersed in a fluid.

In an earlier attempt to solve these technical issues, in 2001, Minh *et al.* presented a probe that could detect the SNOM signal via a hollow micro-machined cantilever glued on top of an optical fiber [9]. In 2011, we proposed to skip the gluing step by directly carving the cantilever out of the cleaved end of the fiber [10], which also adds the possibility to measure the cantilever deflection using fiber interferometry. In that experiment we showed that fiber-top probes can collect the SNOM signal throughout an entire AFM indentation stroke. In 2006, that approach, today known as *fiber-top* technology, had already been used successfully for AFM imaging [11]. However, the manufacturing procedure of both Ming's and our fiber-coupled cantilevers is still rather complex.

In this paper, we propose to approach this problem via a new probe based on *ferrule-top* technology [12]. As illustrated in Fig. 1, ferrule-top probes are obtained by gluing a cantilever to a large glass ferrule equipped with an optical fiber, which can be used to measure the deflection of the cantilever via optical fiber interferometry. A second optical fiber, with a sharp tip on its core, is anchored to the free hanging end of the cantilever to allow light to be transmitted to or from a sample. Thanks to its larger dimensions, the assembly and the fabrication procedures are much simpler than those used in smaller devices, while retaining the advantages of fiber-top probes. We show that, with this approach, which has already been implemented into easy-to-use AFM setups for imaging [13], indentation [14], and transmission scanning microscopy [15], one can obtain high resolution AFM+SNOM images in collection mode both in air and liquids.

Originally, ferrule-top cantilevers were obtained by carving a cantilever on top of a glass ferrule using laser ablation micro-machining [12]. Here we use a new fabrication method that yields better control of the cantilever dimensions, and, therefore, of its properties. The important steps of this approach are illustrated in Fig. 1.

For this experiment the building block of the probe is a 3 x 3 x 7 mm^3 glass ferrule containing a center bore hole with a diameter of 127 μm. The ferrule is initially mounted on a wire cutter (Well Diamantdrahtsagen GmbH, customized

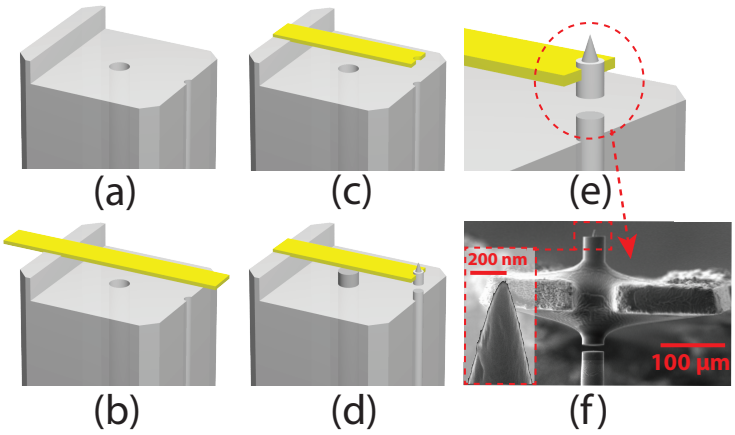

Figure 1: Schematic view of the fabrication process of a ferrule-top probe. (a) Ferrule with ridge, (b) ribbon glued to the ferrule, (c) ribbon micro-machined to create the cantilever, d) complete ferrule-top probe, (e) enlargement of ferrule-top probe, (f) SEM image of the end of the cantilever (front view), insert: magnified tip. See text for details.

for precision machining) to cut a small ridge on one of the facets of the ferrule (Fig. 1 (a)) and a groove on one of the lateral flats to accommodate the tipped fiber. The cantilever is constructed by gluing a glass ribbon (VitroCom Inc.), previously coated with a thin layer of gold, onto the ridge (Fig. 1 (b)). To finalize the cantilever, the probe is mounted on a ps-laser ablation system (Optec System with Lumera Laser source), which is used to cut the ribbon to the desired length and to make a small notch at the extremity to hold the fiber tip (Fig. 1(c)). Typically, a cantilever with a length of 2800 μm, a width of 200 μm and thickness of 30 μm, yealding an approximate spring constant of 6 N/m, is used. A single mode fiber is slid into the center bore hole of the ferrule and glued in place for interferometric detection of the position of the cantilever. The tipped fiber, obtained according to the procedure described in [16], is then glued in the lateral groove and anchored to the cantilever as shown in Fig. 1 (d). At this stage the cantilever is fixed to the probe and unable to move. To release the cantilever, the tipped fiber is cleaved using focused ion beam (FIB) milling (FEI Helios, Ga source). A FIB cut of about 5 μm is sufficient to allow unrestricted bending of the cantilever and still to ensure good light transmission through the gap (Fig. 1 (e)). Since the whole probe is coated with a layer of aluminum, the FIB is also used to create a small aperture at the tip apex to enable light coupling to or from the sample surface. This FIB procedure can be completed within 15 minutes - much less than what is required for creating a fiber-top probe.

The experimental setup, as sketched in Fig. 2, consists of a Dove prism placed under a custom-built AFM system and a ferrule-top probe attached to an XYZ translational stage (Attocube Systems AG). The latter is used to move the probe

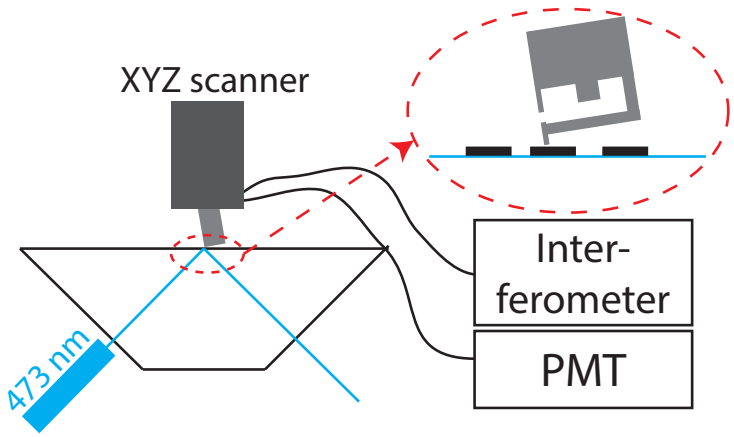

Figure 2: Schematic view of the experimental setup; a shallower angle of incidence was used for measurements in water.

relative to the surface of the prism. A 473 nm, 20 mW laser beam (Changchun New Industries Optomechanics Tech. Co., Ltd.) enters the prism at an incident angle of 45°, creating an evanescent optical field extending just beyond the top surface of the prism. The tip of the ferrule-top probe transfers the optical field into a propagating wave that is guided by the optical fiber to a photo multiplier tube (PMT H9306, Hamamatsu). Simultaneously, the deflection of the cantilever is measured using an interferometer (OP1550, Optics11 B.V. [17]) connected to the end of the central fiber [12, 13].

To demonstrate that the probe works according to design, we mounted a SNOM test grating (SNG01, NT-MDT) on top of the prism. This test sample consists of a thin quartz slide with 20 nm high vanadium diamonds on top. To obtain both SNOM and AFM images simultaneously the probe was raster-scanned in contact mode over the surface of the sample while the optical and topography signal were simultaneously recorded. For the control mechanism, an open source SPM controller (MK3-PLL, SoftDB) and GXSM software [18] were used. To extend the tip lifetime, the system was operated in closed loop.

The evanescent field above the surface of the prism decays exponentially with distance and can be visualized by moving the probe back and forth to the sample surface while recording the optical signal. The tip of a ferrule-top probe thus functions as an antenna that transfers the non-propagating field into a propagating wave. This feature is illustrated in Fig. 3, where we show the light signal collected by the tipped fiber of our probe during a 700 nm indentation stroke in air. In order to increase the signal-to-noise ratio, the laser beam was intensity modulated at a fixed frequency of 1 KHz. The signal was demodulated using a lock-in amplifier set to a time constant of 3 ms.

The moment at which the tip makes contact with the sample is detected by the interferometer, as illustrated in Fig. 3 (b). When the probe retracts, interaction forces between the tip and the surface make the tip stick to the

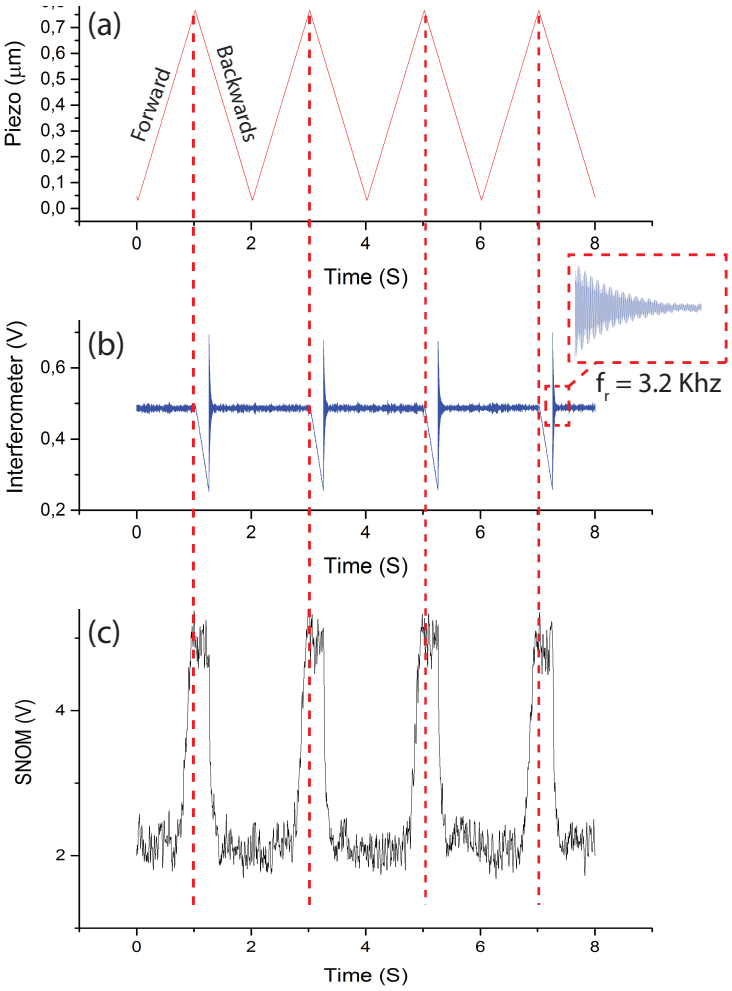

Figure 3: Result of a 700 nm AFM indentation stroke in air. (a) Movement of the piezo in the Z direction, (b) interferometer signal that indicates when the probe is in contact with the surface of the prism, (c) exponential increase of the optical signal when the SNOM tip approaches the evanescent field.

sample causing the interferometer signal to decrease. The vibration, which illustrates the resonance frequency f_r of the probe, indicates the moment that the tip loses contact with the surface. As expected, during the contact period, the optical signal remains constant. It is also clear that no SNOM signal is present when the tip is far away from the sample surface and outside the range of the evanescent field.

More importantly, using this technique, near-field imaging with a lateral resolution beyond the diffraction limit is feasible. Since the tip can only detect the near-field light when it is in close proximity with an object, and rejects most of the far field radiation, the lateral resolution of an obtained image mainly depends on the tip size, rather than the wavelength of the laser. In Fig. 4 we show AFM and SNOM images of a standard test grating that were recorded simultaneously. The SNOM signal was obtained in collection mode. The size of the scan area was 8 x 8 μm^2 with an image resolution of 256 x 256 pixels. An excellent contrast between the vanadium structure (dark) and the quartz substrate (light) illustrates the capabilities of this system and demonstrates the potential of ferrule-top probes. Due to the FIB cut, one may expect interference noise to occur because of the cavity created in the gap. This phenomenon would not affect the image because the instrument works in closed loop contact mode. Furthermore, we did not observe this artifact to occur, even when operating in open loop.

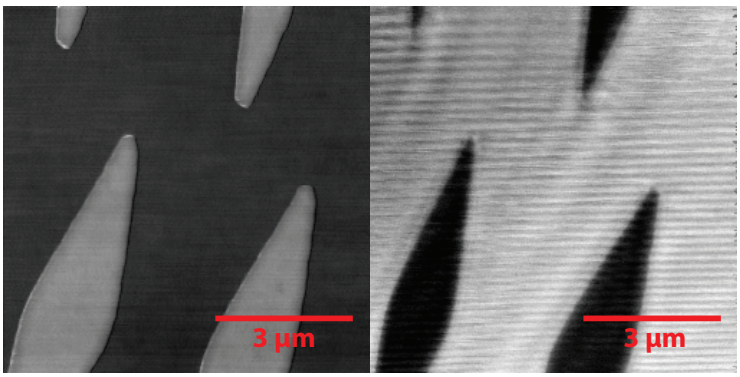

Figure 4: 8 x 8 μm^2 (a) AFM and (b) SNOM contact mode images of the NT-MDT SNG01 test grating (256 x 256 pixels).

Fig. 5 shows images of a small part of the same sample with dimensions 4,4 x 2,2 μm^2, which can be used to estimate the lateral resolution of our imaging system. In the line profile, as the tip is scanned across a steep edge, the distance between the beginning and the end point of the edge was measured. The approximate resolution was 45 nm in AFM mode and 160 nm in SNOM mode, in good agreement with what was expected from the size of the aperture. The observed edge is of course given by the convolution of the dimensions of

the tip and the physical width of the edge. However, an independent AFM measurement using a commercial system with a 10 nm tip (Fastscan, Bruker Co., Ltd.) showed the edge to be negligible.

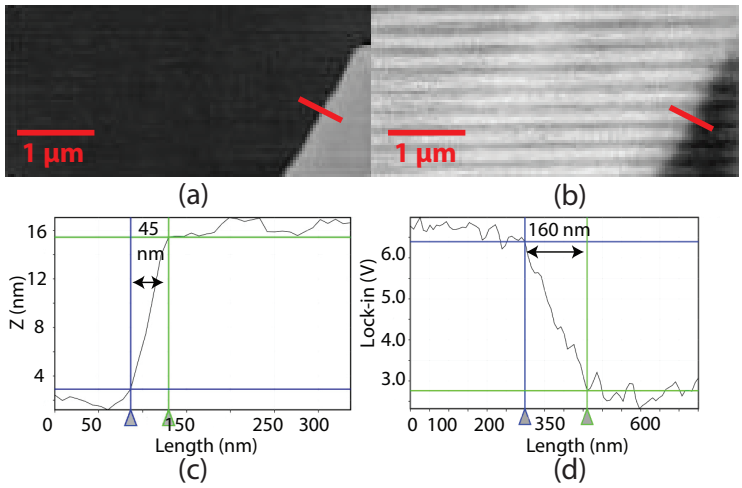

Figure 5: (a) AFM and (b) SNOM contact mode images of a small 4,4 x 2,2 μm^2 area. Graphs (c) and (d) show the line profile of the edge of the vanadium structure

In the SNOM images, one can clearly differentiate a periodic horizontal pattern. The blue laser beam impinges the top surface of the prism at 45°, which means that light reflected from the opposite end of the prism arrives at the exact same point on the surface. The two beams interfere with each other creating a standing wave of period 209 ± 22 nm as shown in Fig. 6. The presence of interference lines in SNOM imaging was earlier observed by Meixner *et al.* [19], who showed that the period Λ of the interference fringes can be calculated using:

$$\Lambda = \frac{\lambda_0}{2n \sin\theta} \tag{1}$$

where λ_0, θ and n are the laser wavelength, incident angle and the refractive index of the prism respectively. In our experiment, $\lambda_0 = 473$ nm, $\theta = 45°$ and $n = 1.51$. Substituting in eq. 1, a theoretical period of 212 nm is obtained, which is in agreement with the experimental value.

A major advantage of ferrule-top technology can be found in a comparable performance and easy operation in air and liquids. To investigate the performance of our SNOM probe in liquid, the test grating was fully immersed in water. To create a suitable evanescent field, the incident angle of the laser had to be adjusted to be higher than the critical angle of the glass-water interface, which is 62°. Fig. 7 shows the images of the same test grating, fully immersed in water. It is clear that the probe works with a similar performance as in air.

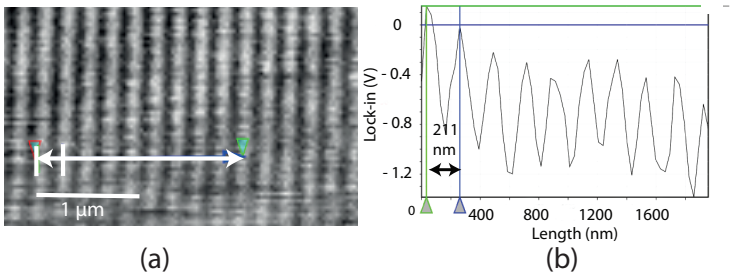

Figure 6: Detail of the interference pattern created by the two interfering beams (reversed scanning direction). (a) 4 x 2 μm^2 image, (b) line scan showing the periodic wave.

Interestingly, these images do not show the characteristic interference fringes as mentioned before. This can be explained by the different incident angle of the laser beam. In this configuration, light is not reflected back to the same spot and therefore no interference takes place.

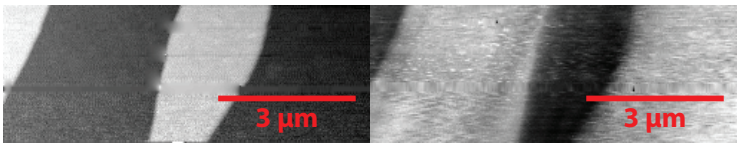

Figure 7: (a) AFM and (b) SNOM contact mode images of the NT-MDT test grating measured in water.

In conclusion, we have shown that ferrule-top technology allows one to obtain SNOM and topographic images of a test grating simultaneously with a resolution comparable to conventional SNOM systems, both in air and water. This result paves the way for better AFM+SNOM imaging of biological samples and for other AFM+SNOM applications in critical environments.

The research leading to these results has received funding from LASERLAB-EUROPE (grant agreement no. 284464, EC's Seventh Framework Programme), ERC (grant agreement no. 201739, EC's Seventh Framework Programme (FP7/2007-2013)) and NanonextNL (project no. 9A#13).

References

[1] N. Jalili and K. Laxminarayana, Mechatronics **14**, 907–945 (2004).

[2] H. Heinzelmann and D. W. Pohl, Applied Physics A **59**, 89101 (1994).

[3] B. Hecht, B. Sick, U. P. Wild, V. Deckert, R. Zenobi, O. J. F. Martin, and D. W. Pohl, The Journal of Chemical Physics **112**, 7761 (2000).

[4] J. Kim and K.-B. Song, Micron **38**, 409–426 (2007).

[5] C. Höppener, D. Molenda, H. Fuchs, and A. Naber, Journal of microscopy **210**, 288293 (2003).

[6] M. Koopman, A. Cambi, B. de Bakker, B. Joosten, C. Figdor, N. van Hulst, and M. Garcia-Parajo, FEBS Letters **573**, 6–10 (2004).

[7] H. Muramatsu, N. Chiba, N. Yamamoto, K. Homma, T. Ataka, M. Shigeno, H. Monobe, and M. Fujihira, Ultramicroscopy **71**, 73–79 (1998).

[8] C. Mihalcea, W. Scholz, S. Werner, S. Mnster, E. Oesterschulze and R. Kassing, Applied physics letters, **68**, 35313533 (1996).

[9] P. N. Minh, T. Ono, H. Watanabe, S. S. Lee, Y. Haga, and M. Esashi, Applied Physics Letters **79**, 3020 (2001).

[10] B. Tiribilli, G. Margheri, P. Baschieri, C. Menozzi, D. Chavan, and D. Iannuzzi, Journal of Microscopy **242**, 10–14 (2011).

[11] D. Iannuzzi, S. Deladi, V. J. Gadgil, R. G. P. Sanders, H. Schreuders, and M. C. Elwenspoek, Applied Physics Letters **88**, 053501 (2006).

[12] G. Gruca, S. De Man, M. Slaman, J. H. Rector, and D. Iannuzzi, Measurement Science and Technology **21**, 094033 (2010).

[13] D. Chavan, G. Gruca, S. de Man, M. Slaman, J. H. Rector, K. Heeck, and D. Iannuzzi, Review of Scientific Instruments **81**, 123702 (2010).

[14] D. Chavan, T. C. van de Watering, G. Gruca, J. H. Rector, K. Heeck, M. Slaman, and D. Iannuzzi, Review of Scientific Instruments **83**, 115110 (2012).

[15] D. Chavan, G. Gruca, T. van de Watering, K. Heeck, J. Rector, M. Slaman, D. Andres, B. Tiribilli, G. Margheri, and D. Iannuzzi, Conf. of Optical Micro- and Nanometrology (2012).

[16] T. Pangaribuan, K. Yamada, S. Jiang, H. Ohsawa, and M. Ohtsu, Japanese Journal of Applied Physics **31**, L1302–L1304 (1992).

[17] Declaration of interest: D. Iannuzzi is share-holder of Optics11 B.V.

[18] P. Zahl, M. Bierkandt, S. Schroder, and A. Klust, Review of Scientific Instruments **74**, 1222–1227 (2003).

[19] A. J. Meixner, M. A. Bopp, and G. Tarrach, Applied optics **33**, 79958000 (1994).